Available online at www.sciencedirect.com
ScienceDirect
Mechanical Systems and Signal Processing 21 (2007) 3072–3087
Mechanical Systems and Signal Processing
www.elsevier.com/locate/jnlabr/ymssp

Blind source separation based vibration mode identification

Wenliang Zhou[a,*], David Chelidze[b]

[a]Lang Mekra North America, LLC., 101 Tillessen Blvd, Ridgeway, SC 29130, USA
[b]Department of Mechanical Engineering & Applied Mechanics, University of Rhode Island, Kingston, RI 02881, USA

Received 18 January 2007; received in revised form 24 March 2007; accepted 25 May 2007
Available online 17 June 2007

Abstract

In this paper, a novel method for *linear normal mode* (LNM) identification based on *blind source separation* (BSS) is introduced. Modal coordinates are considered as a specific case of sources that have certain time structure. This structure makes modal coordinates identifiable by many BSS algorithms. However, algorithms based on second-order statistics are particularly suited for extracting LNMs of a vibration system. Two well-known BSS algorithms are considered. First, *algorithm for multiple unknown signals extraction* (AMUSE) is used to illustrate the similarity with *Ibrahim time domain* (ITD) modal identification method. Second, *second order blind identification* (SOBI) is used to demonstrate noise robustness of BSS-based mode shape extraction. Numerical simulations and experimental results from these BSS algorithms and ITD method are presented.

Keywords: Modal analysis; Blind source separation; Independent component analysis; Vibration tests

1. Introduction

Blind source separation (BSS), or closely related algorithm called *independent component analysis* (ICA), deals with recovering a set of underlying sources from observations without knowing mixing processing and sources. These methods were originally introduced in the context of neural network modeling [1] and have been shown tremendous applications in various fields including: image processing [2], biomedical data analysis [3], telecommunications [4] and stock analysis [5]. In the past several years, an increasing number of the applications of BSS or ICA to structural dynamics have been found in technical publications. Some examples of these are signal separation from convoluted mixing sources for bearing diagnosis [7], robust extraction of rotating machinery signals in noisy environments [8], compression of experimental data for further damage identification [6], identification of particular machine signals from complex machinery sensor measurements [9], etc. The purpose of this paper is to study the application of BSS in the extraction of LNMs of a vibration system. In particular, mode shape extraction in noisy environments is emphasized.

Conventional linear modal analysis decomposes displacement matrix into a mode shape matrix and a modal coordinate matrix. Modal coordinates express separated fundamental oscillations, while mode shapes

*Corresponding author. Tel.: +1 803 337 4922.
E-mail addresses: zhouwl@gmail.com (W. Zhou), chelidze@egr.uri.edu (D. Chelidze).

0888-3270/$ - see front matter © 2007 Elsevier Ltd. All rights reserved.
doi:10.1016/j.ymssp.2007.05.007

mathematically describe the participation of each oscillation in the output (displacement matrix). Current time domain modal parameter identification methods [10–13] are based on closed-form solutions to an idealized, deterministic, linear vibratory system. However, the accuracy of results depends on the validity of mathematical model of data and deteriorates drastically when noise is present. Here an alternative approach is advocated, which is to formulate the modal identification as a BSS problem, and to employ multivariate analysis to separate each independent oscillation. As a result, the mixing matrix will provide mode shape information and the separated oscillations will contain the associated natural frequencies and damping ratios. In fact, some of the BSS algorithms even have similar steps to current time domain modal analysis. These steps include: eigenvalue decomposition or generalized eigenvalue decomposition, time shifting technique, construction of covariance and cross-covariance matrices, etc.

The paper is organized as follows: the general theory of BSS is introduced in Section 2. Section 3 explains mode shape extraction from the viewpoint of BSS. One of BSS algorithms, *algorithm for multiple unknown signals extraction* (AMUSE), is examined in detail and compared to a well-known time domain modal analysis method, Ibrahim time domain (ITD) method. The similarity and relationship between two different problems are explained. Another BSS algorithm, *second order blind identification* (SOBI), is used to demonstrate the noise robustness of the BSS-based mode shape extraction. In Section 4, numerical and experimental results from the BSS-based algorithms and conventional ITD method are given. In Section 5, we talk about frequency and damping extraction and concerns regarding practical applications of the proposed method and conclude the paper.

2. A brief overview of the BSS theory

2.1. A problem statement

BSS is an emerging technique for signal processing and data analysis. Given a series of observed signals, BSS aims at recovering the underlying sources by exploiting the assumption of their mutual independence. Depending upon the type of mixing, BSS can be classified as linear [15,16] or nonlinear [17], where the mixtures are linear or nonlinear combinations, respectively, of the sources. Additional classifications include linear simultaneous mixing [15,16] or convolutive mixing [18,19], which can be further subclassified as blind deconvolution or blind equalization. BSS model considered in this paper is a linear simultaneous mixture formulated as

$$\mathbf{x} = \mathbf{A}\mathbf{s} + \mathbf{n}, \tag{1}$$

where $\mathbf{x} = [x_1, x_2, \ldots, x_m]^T \in \mathbb{R}^m$ is a vector containing measured scalar signals x_i, $\mathbf{s} = [s_1, s_2, \ldots, s_n]^T \in \mathbb{R}^n$ is a vector containing original sources ($m \geqslant n$), $\mathbf{A} \in \mathbb{R}^{m \times n}$ is an unknown mixing matrix with full column rank and $\mathbf{n} \in \mathbb{R}^m$ represents additive measurement noise. For simplicity, the discussion here is restricted to the case of $m = n$. The goal of BSS is to find a demixing matrix $\mathbf{A}^{-1}$, such that $\mathbf{A}^{-1}\mathbf{x}$ recovers the underlying sources $\mathbf{s}$ using measured $\mathbf{x}$. A schematic illustration of BSS process is given in Fig. 1.

2.2. Basic assumptions

Due to the blindness of the problem, certain assumptions about sources are needed to proceed with the analysis. The most general assumption in BSS or ICA is to assume the sources are mutually independent. In other words, the joint probability density of the sources should be factorizable into the product of their marginal densities as

$$p_{s_1,s_2,\ldots,s_n}(s_1, s_2, \ldots, s_n) = p_{s_1}(s_1)p_{s_2}(s_2)\cdots p_{s_n}(s_n), \tag{2}$$

where $p_{s_1,s_2,\ldots,s_n}(s_1, s_2, \ldots, s_n)$ is the joint probability density and $p_{s_i}(s_i)$ represents each marginal density. This is a theoretically strong but practically natural assumption for many applications. Secondly, sources are generally assumed to be non-Gaussian or to have at most one Gaussian signal. Thirdly, the mixing matrix $\mathbf{A}$ is assumed to be full column rank but is otherwise unknown. However, these general assumptions can sometimes be relaxed when dealing with signals of specific characteristics. For example, if the sources are time signals the

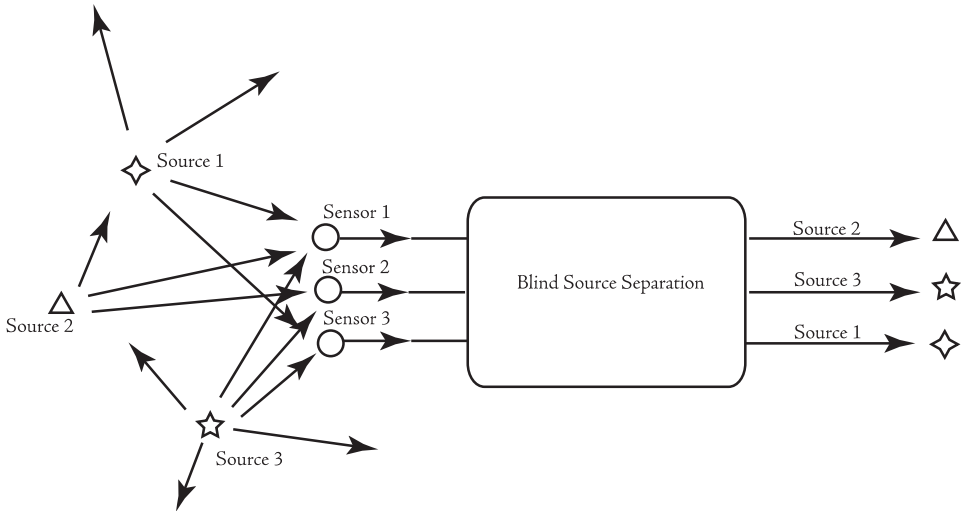

Fig. 1. The framework of BSS.

mutual independence can be relaxed to mutual uncorrelation. In addition, for time signals, the Gaussian distribution is also not required. Classical vibration modal analysis deals with vibration signals that have time structure.

2.3. Indeterminacy of the BSS

With the above assumptions BSS is solvable with two inherent ambiguities. Firstly, the order of the estimated sources is not identifiable, as any permutation of these sources is also a solution. Secondly, we cannot determine the original variance of sources since in Eq. (1) $\mathbf{x}$ is the only known variable, and any scaling of sources can be canceled by inverse scaling of the associated components of matrix $\mathbf{A}$. Therefore, generally, all sources are assumed to have unit variances.

2.4. Solution strategy

ICA or BSS is essentially an optimization problem, which can be solved if appropriate objective function, constraint (e.g., unit variance of sources) and numerical algorithm are employed. The objective functions are usually chosen as some measurement of non-Gaussianity or independence of the sources, such as the Kurtosis or fourth-order cumulant [21] statistics, Negentroy [22], likelihood [23], etc. The optimization methods range from the classical gradient descent method or Newton-like algorithms [1] to fast fixed-point algorithm [22] or joint diagonalization [16,21]. Most ICA or BSS algorithms start with preprocessing steps, which usually include centering (removal of mean values from measurements) and whitening (basically, PCA). They are intended to reduce noise level and avoid over-learning as well as to improve convergence properties.

When the sources are time signals, we can make use of time structure to achieve the desired source separation. To this end various methods have been developed, such as AMUSE [15], SOBI [16], *temporal decorrelation separation* (TDSEP) [24] or *time–frequency blind source separation* (TFBSS) [25]. Among these methods, AMUSE, SOBI and TDSEP are quite similar in basic theory, since all of them exploit the information contained in auto- and cross-covariance matrices. TFBSS, in contrast, examines the non-stationarity of the signals and uses the auto- and cross-time-frequency distribution matrix to extract independent sources. All these methods employ the technique of joint-diagonalization of matrices. In this paper, measured signals are assumed to be stationary, thus TFBSS is not discussed here. Since AMUSE and SOBI can be closely related with current time domain modal analysis methods and TDSEP is essentially the same as SOBI when dealing with time signals, focuses will be on AMUSE and SOBI algorithms in the following discussion.

3. Mode shape extraction and BSS

Modal parameter identification consists of extracting a set of natural frequencies, damping factors and mode shapes of a structure. Among these parameters, mode shapes provide mathematical description of deflection patterns of vibration when the system vibrates at one of the natural frequencies. Viewed from another point, mode shapes describe the participation of each independent oscillation in the output response.

Considering a classical modal analysis, governing equations of motion for an n-degree-of-freedom free linear vibration system can be written as

$$\mathbf{M}\ddot{\mathbf{x}} + \mathbf{C}\dot{\mathbf{x}} + \mathbf{K}\mathbf{x} = \mathbf{0}, \tag{3}$$

where $\mathbf{M}$, $\mathbf{C}$ and $\mathbf{K} \in \mathbb{R}^{n\times n}$ are mass, damping and stiffness matrices, respectively, $\ddot{\mathbf{x}}$, $\dot{\mathbf{x}}$ and $\mathbf{x} \in \mathbb{R}^n$ are acceleration, velocity and displacement vectors. The free decay (or transient) oscillations for proportionally or lightly damped system can be described as

$$\mathbf{x}(t) = \sum_{i=1}^{n} \boldsymbol{\psi}_i a_i \exp(-\xi_i t)\cos(\omega_i t + \varphi_i), \tag{4}$$

ξ_i, ω_i, φ_i represent damping ratio, natural frequency and phase angle, respectively, $\boldsymbol{\psi}_i$, a_i are constants, and t is time. Eq. (4) can be written in a matrix form:

$$\mathbf{x}(t) = \boldsymbol{\Psi}\mathbf{Q}(t), \tag{5}$$

where $\mathbf{x}(t)$ is the output vibration displacement, $\boldsymbol{\Psi} \in \mathbb{R}^{n\times n}$ is the mode shape matrix composed of mode shapes $\boldsymbol{\psi}_i$, and $\mathbf{Q}(t) \in \mathbb{R}^n$ is vector containing modal coordinates $a_i \exp(-\xi_i t)\cos(\omega_i t + \varphi_i)$. Many time domain modal parameter identification involves extracting mode shape matrix $\boldsymbol{\Psi}$ and natural frequencies ω_i and damping ratios ξ_i contained in $\mathbf{Q}(t)$ by using only the output signal $\mathbf{x}(t)$. Assuming the output signals are sampled every Δt time period and a total of m data points are recorded for each component of $\mathbf{x}$, then Eq. (5) can be written as

$$\mathbf{X} = \boldsymbol{\Psi}\mathbf{Q}, \tag{6}$$

where $\mathbf{X} \in \mathbb{R}^{n\times m}$ is the trajectory matrix composed of the sampled components of $\mathbf{x}$, and $\mathbf{Q} \in \mathbb{R}^{n\times m}$ is a matrix of corresponding modal coordinates.

Similarities between the time domain modal analysis and BSS can be seen as: both deal with estimating the underlying components from mixed signals. BSS algorithms use only the output information and many time domain modal analysis methods also can handle output-only situation. The modal coordinates $\mathbf{Q}(t)$ are a special case of general sources $\mathbf{s}$ with time structure. Furthermore, distinct modal coordinates automatically meet the requirement of uncorrelation of sources in BSS. Most BSS algorithms focus on finding the demixing matrix $\mathbf{A}^{-1}$ and many sophisticated algorithms which are robust to noise have been proposed. These algorithms could also be implemented to extract mode shape information of a vibration system in noisy environments. Fig. 2 shows the schematic illustration of mode extraction process based on BSS. The signals on the left-hand side are output vibration signals and the signals on the right-hand side are the separated modes. As is mentioned earlier, AMUSE, SOBI and TDSEP use second-order statistics by constructing auto- and cross-covariance matrices and simultaneously diagonalize these matrices to estimate the underlying mixing matrix. This analytical procedure is quite similar to current time domain modal analysis methods, for example

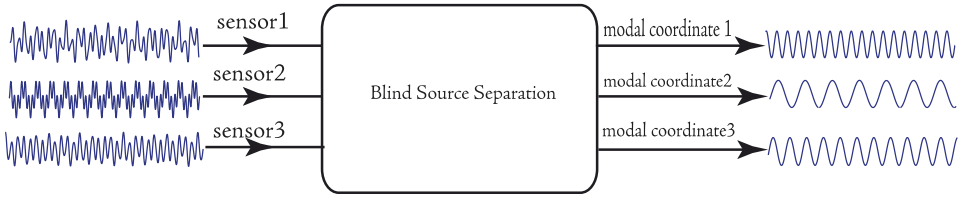

Fig. 2. BSS in mode extraction.

ITD method can be described as a generalized eigenvalue decomposition of measured signals' auto- and cross-covariance matrices [26].

3.1. AMUSE and mode shape extraction

AMUSE was introduced by Tong et al. in 1991 [15] and can handle Gaussian sources. AMUSE exploits the second-order statistics of the mixed signals and performs an eigenvalue decomposition to the time-lagged covariance matrix. The specific procedures are:

- Centering and whitening of the mixed signal matrix to get $\mathbf{Z}_t$, $\mathbf{Z}_t = \mathbf{P}\mathbf{X}_t$, $\mathbf{P}$ is the whitening matrix, and subscript t is used to describe a particular time sequence.
- Calculating the eigenvalue decomposition of $\hat{\mathbf{R}}_z = \frac{1}{2}[\mathbf{R}_z + \mathbf{R}_z^T]$, where $\mathbf{R}_z = E[\mathbf{Z}_t\mathbf{Z}_{t+\tau}^T]$ is a time-lagged covariance matrix, E represents expectation value, and τ is some time delay.
- The estimated mixing matrix is obtained as $\hat{\mathbf{A}} = \mathbf{P}^{-1}\mathbf{U}$, where $\mathbf{U}$ is the eigenvector matrix of $\hat{\mathbf{R}}_z$ from the second step.

The whitening is usually done by performing PCA of the original mixed signals, $\mathbf{X}_t$ for instance. If the eigenvalue decomposition of the covariance matrix of $\mathbf{X}_t$ is $\mathbf{R}_x = \mathbf{V}\mathbf{D}\mathbf{V}^T$, $\mathbf{D}$ is the eigenvalue matrix and $\mathbf{V}$ is the eigenvector matrix, then the whitening matrix is $\mathbf{P} = \mathbf{D}^{-1/2}\mathbf{V}^T$ and the estimated mixing matrix is $\hat{\mathbf{A}} = \mathbf{V}\mathbf{D}^{1/2}\mathbf{U}$.

Looking at the procedure of AMUSE, one obvious difference between BSS and the above-mentioned time domain modal analysis algorithms is that the latter do not have the centering and whitening steps, while AMUSE and most BSS algorithms do. However, we will show these steps are implicitly included in the time domain modal analysis.

Firstly, let us take a look at the step of centering. ITD and other time domain modal analysis methods start analysis of signals with a form of Eq. (4). The means of these signals are automatically zeros. In fact, if the means of the signals are not zeros due to noise or other effects, these methods will give misleading results.

Next, for the step of whitening, we say this has been included in current time domain modal analysis by a generalized eigenvalue decomposition. In other words, the separated steps of whitening and an eigenvalue decomposition of whitened matrix in BSS can be combined by performing a generalized eigenvalue decomposition.

Taking AMUSE as an example, after centering and whitening we have the signal matrix as

$$\mathbf{Z}_t = \mathbf{D}^{-1/2}\mathbf{V}^T\mathbf{X}_t \tag{7}$$

and

$$\begin{aligned}\hat{\mathbf{R}}_z &= \tfrac{1}{2}[\mathbf{R}_z + \mathbf{R}_z^T] \\ &= \tfrac{1}{2}\mathbf{D}^{-1/2}\mathbf{V}^T[\mathbf{X}_t\mathbf{X}_{t+\tau}^T + \mathbf{X}_{t+\tau}\mathbf{X}_t^T]\mathbf{V}\mathbf{D}^{-1/2}\end{aligned} \tag{8}$$

or

$$\hat{\mathbf{R}}_z = \mathbf{D}^{-1/2}\mathbf{V}^T\hat{\mathbf{R}}_x\mathbf{V}\mathbf{D}^{-1/2}, \quad \text{where } \hat{\mathbf{R}}_x = \tfrac{1}{2}(\mathbf{X}_t\mathbf{X}_{t+\tau}^T + \mathbf{X}_{t+\tau}\mathbf{X}_t^T). \tag{9}$$

The eigenvalue decomposition to the matrix $\hat{\mathbf{R}}_z$ is

$$\hat{\mathbf{R}}_z = \mathbf{U}\mathbf{\Lambda}\mathbf{U}^T, \tag{10}$$

where $\mathbf{\Lambda}$ is the eigenvalue matrix of $\hat{\mathbf{R}}_z$.

Substituting Eq. (9) into Eq. (10):

$$\mathbf{D}^{-1/2}\mathbf{V}^T\hat{\mathbf{R}}_x\mathbf{V}\mathbf{D}^{-1/2} = \mathbf{U}\mathbf{\Lambda}\mathbf{U}^T, \tag{11}$$

post-multiply both sides by $\mathbf{D}^{-1/2}\mathbf{V}^T$:

$$\mathbf{D}^{-1/2}\mathbf{V}^T\hat{\mathbf{R}}_x\mathbf{V}\mathbf{D}^{-1}\mathbf{V}^T = \mathbf{U}\mathbf{\Lambda}\mathbf{U}^T\mathbf{D}^{-1/2}\mathbf{V}^T, \tag{12}$$

and pre-multiply both sides by $\mathbf{U}^T$, we have

$$\mathbf{U}^T\mathbf{D}^{-1/2}\mathbf{V}^T\hat{\mathbf{R}}_x\mathbf{V}\mathbf{D}^{-1}\mathbf{V}^T = \mathbf{\Lambda}\mathbf{U}^T\mathbf{D}^{-1/2}\mathbf{V}^T. \tag{13}$$

Setting $\mathbf{L}^T = \mathbf{U}^T\mathbf{D}^{-1/2}\mathbf{V}^T$ and noticing that $\mathbf{V}\mathbf{D}^{-1}\mathbf{V}^T = \mathbf{R}_x^{-1}$, Eq. (13) becomes

$$\mathbf{L}^T\hat{\mathbf{R}}_x = \mathbf{\Lambda}\mathbf{L}^T\mathbf{R}_x \tag{14}$$

or

$$\hat{\mathbf{R}}_x\mathbf{L} = \mathbf{R}_x\mathbf{L}\mathbf{\Lambda}. \tag{15}$$

Now we can see $\mathbf{L}$ is actually the generalized eigenvector matrix of Eq. (15). Since $\mathbf{L}^{-T} = \mathbf{V}\mathbf{D}^{1/2}\mathbf{U} = \hat{\mathbf{A}}$, we say the inverse and transpose of the generalized eigenvector matrix of matrix pair ($\hat{\mathbf{R}}_x$, $\mathbf{R}_x$) provides the mixing matrix. This result corresponds well with ITD formed as a generalized eigenvalue decomposition. $\mathbf{L}$ provides mode shape information. As is shown in Ref. [26], LSCE [12], ERA [11] can all be formulated as a generalized eigenvalue decomposition of different matrix pairs, and the generalized eigenvector matrix provides mode shape information. The above demonstrates that AMUSE essentially has the same form as ITD and there is no whitening step either, if formulated using generalized eigenvalue decomposition.

As for the symmetry of the cross-covariance matrix $\hat{\mathbf{R}}_x$, this is associated with the number of the dimension for the reconstructed signal matrix. In ITD the analytic matrix needs to be reconstructed into $2n$ dimensions (where n is the number of degree-of-freedom) to account for the complex conjugate modal parameters. This is because ITD aims to find exact solution by taking advantage of mathematical form of the output signals. AMUSE, however, is based on statistical analysis and works with whatever the real dimension of the mixture is. The technique of simultaneous diagonalization the auto- and cross-covariance matrices is the essence in AMUSE or other BSS algorithms. If the cross-covariance matrix is not symmetric, not only the extracted mixing matrices are sometimes complex but also the desired simultaneous diagonalization of matrix pair by a single matrix is not possible. Essentially, for a non-symmetric matrix pair case we need to use both the right and left generalized eigenvector matrices to realize simultaneous diagonalization. The use of symmetric form in BSS algorithms provides a possibility of using a single real diagonalization matrix to best approximate both the left and right eigenvector matrices.

3.2. SOBI and mode shape extraction

SOBI algorithm was introduced by Belouchrani et al. in 1997 [16] and is an extension of AMUSE. It is intended to overcome the shortcoming of AMUSE, when the time lag τ is unfortunately chosen to result in two similar eigenvalues and lead to the unidentifiability of sources. Compared with AMUSE, SOBI proposes to simultaneously diagonalize several time-lagged covariance matrices with different time lags τ. Using off function to describe a diagonalization of matrix $\mathbf{B}$:

$$\mathrm{off}(\mathbf{B}) = \sum_{1\leqslant i\neq j\leqslant n} |B_{ij}|^2, \tag{16}$$

the simultaneous diagonalization of p matrices becomes an optimization problem with respect to a matrix $\mathbf{G}$, such that the sum of all the off-diagonal terms in $\mathrm{off}(\mathbf{B}_i)$, $(i = 1,\ldots,p)$ is minimum:

$$\min_{\mathbf{G}} \sum_{i=1}^{p} \mathrm{off}(\mathbf{G}^T\mathbf{B}_i\mathbf{G}). \tag{17}$$

Numerical algorithm based on *Jocobi rotation* technique was provided to implement the joint diagonalization in the original paper [16]. The procedures of SOBI are the same as AMUSE, except the step of eigenvalue decomposition of time-lagged covariance $\hat{\mathbf{R}}_z$ is replaced by joint diagonalization of several time-lagged covariance matrices with different time lags τ_i. In addition to the reduction of the possibility of unidentifiability of $\mathbf{L}$, SOBI appears to be much more robust to noise than AMUSE. Thus, when applied to linear normal mode identification, SOBI has similar physical explanation as AMUSE but the results are expected to be more stable and robust.

4. Numerical and experimental results

In this section, numerical and experimental results for extracting LNMs by AMUSE, SOBI and ITD are provided.

Firstly, numerical simulations of a three-degree-of-freedom vibration system with and without damping in noise-free and noisy environments are examined. In particular, noisy environment is emphasized to show the robustness of the BSS-based methods over the conventional ITD method. We also consider the effect of signal preprocessing (PCA analysis) on mode shape extraction, which is used in current time domain methods.

4.1. Noise-free vibration system

4.1.1. Undamped free vibration case

The first example is an undamped three-degree-of-freedom discrete-parameter system vibrating under initial excitations. The setup of the system is shown in Fig. 3. The governing equation of the system is

$$\mathbf{M}\ddot{\mathbf{x}} + \mathbf{K}\mathbf{x} = 0 \quad \text{where } \mathbf{M} = \begin{bmatrix} 2 & 0 & 0 \\ 0 & 1 & 0 \\ 0 & 0 & 1 \end{bmatrix}, \quad \mathbf{K} = \begin{bmatrix} 2 & -1 & 0 \\ -1 & 2 & -1 \\ 0 & -1 & 1 \end{bmatrix}. \tag{18}$$

The initial displacements are $\mathbf{x}(0) = [1, 0, 0]^T$ and the initial velocities are $\mathbf{v}(0) = [0, 0, 0]^T$. The sampling time in the simulation is 0.1 s and a total of 2000 points are used. The LNMs from vibration theory are calculated as

$$\mathbf{\Psi} = \begin{bmatrix} 0.3602 & 0.7071 & 0.2338 \\ 0.5928 & 0.0000 & -0.8524 \\ 0.7204 & -0.7071 & 0.4676 \end{bmatrix}, \tag{19}$$

where each column represents a modal vector which has been normalized to have unitary norm. The errors of mode shape approximation are described by *Er*, which is the *Euclidian distance* of two mode shape vectors, and the Modal Assurance Criterion (MAC). The mathematical expressions are given as

$$Er_i = \|\boldsymbol{\psi}_i - \bar{\boldsymbol{\psi}}_i\|_2 \quad \text{and} \quad \text{MAC}_i = \frac{(\boldsymbol{\psi}_i^T \bar{\boldsymbol{\psi}}_i)^2}{(\boldsymbol{\psi}_i^T \boldsymbol{\psi}_i)(\bar{\boldsymbol{\psi}}_i^T \bar{\boldsymbol{\psi}}_i)}, \tag{20}$$

where $\boldsymbol{\psi}_i$ and $\bar{\boldsymbol{\psi}}_i$ represent ith theoretical and estimated mode vectors, respectively.

After obtaining the output displacement signals from Eq. (18), AMUSE and SOBI analysis are performed. In Fig. 4, the separated sources or modal coordinates from AMUSE and SOBI are provided. Table 1 lists the results of mode shape extraction from AMUSE, SOBI, and ITD. *Er* and MAC are calculated between these methods and the theoretical results. The subscripts 1, 2 and 3 in the first row represent first mode, second mode and third mode in the example.

For SOBI algorithm, a simultaneous diagnolization of 50 time-lagged covariance matrices with delay time from 1 sampling unit to 50 sampling units is used.

As expected, ITD method provides exact solution, while AMUSE and SOBI give approximated results from statistical viewpoint. However, these approximations are acceptably good.

4.1.2. Damped free vibration case

When damping is present, mode shapes are generally composed of complex conjugate vectors which include both the amplitude and phase angle information. The BSS-based mode shape identification, however, gives us

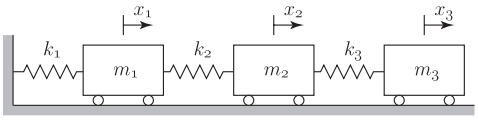

Fig. 3. A three-degree-of-freedom undamped vibration system.

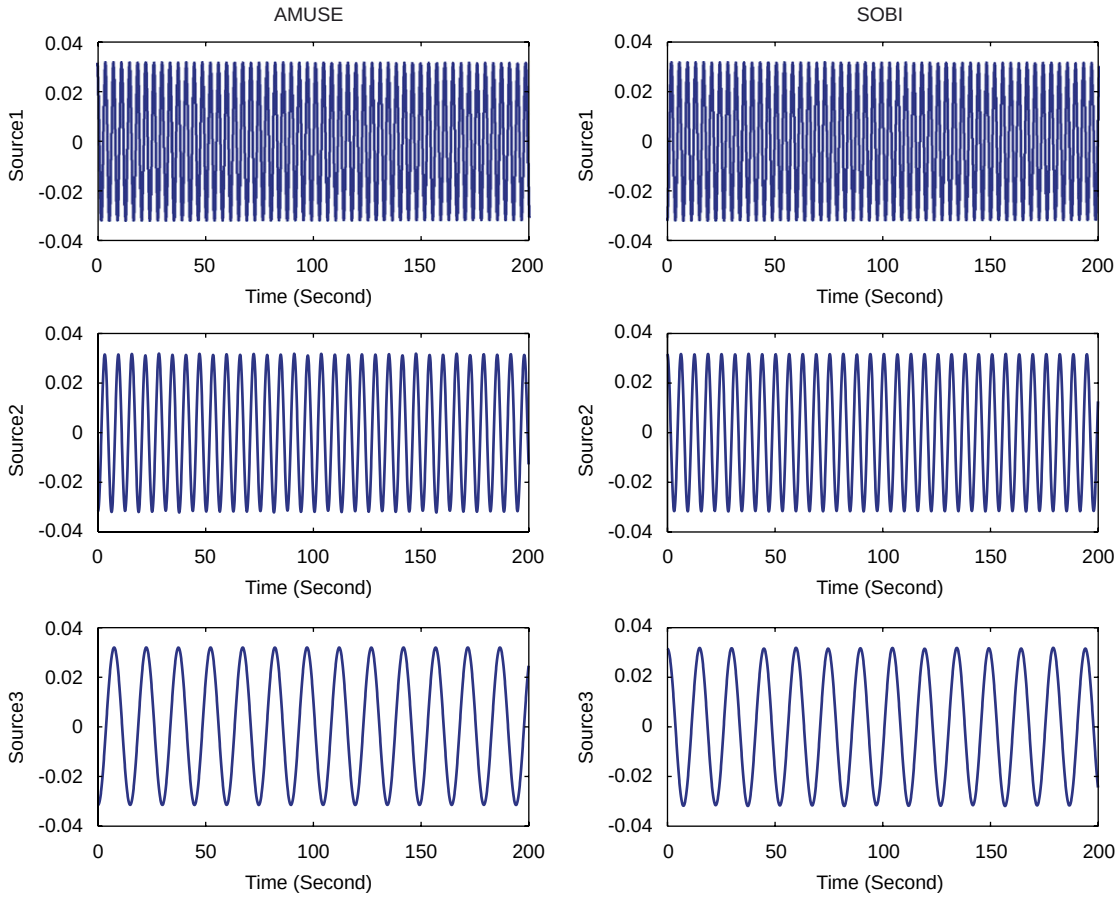

Fig. 4. Separated sources from AMUSE and SOBI. Left column represents results from AMUSE and right column gives results from SOBI.

Table 1
Errors of mode shape extraction (undamped)

	Er_1 (MAC_1)	Er_2 (MAC_2)	Er_3 (MAC_3)
AMUSE	0.0120 (0.99)	0.0009 (1.00)	0.0112 (0.99)
SOBI	0.0023 (1.00)	0.0039 (1.00)	0.0045 (1.00)
ITD	0.0000 (1.00)	0.0000 (1.00)	0.0000 (1.00)

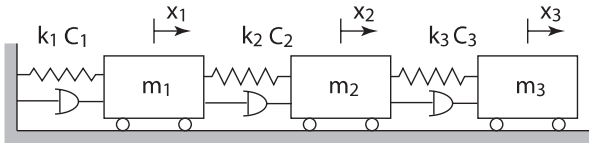

Fig. 5. A three-degree-of-freedom damped vibration system.

the amplitude information since we consider the linear simultaneous mixing case. Again, we use the same vibration system as the previous case, except that damping is added as it is shown in Fig. 5. The modal damping ratios are 0.12, 0.05, 0.03, and other parameters are kept the same.

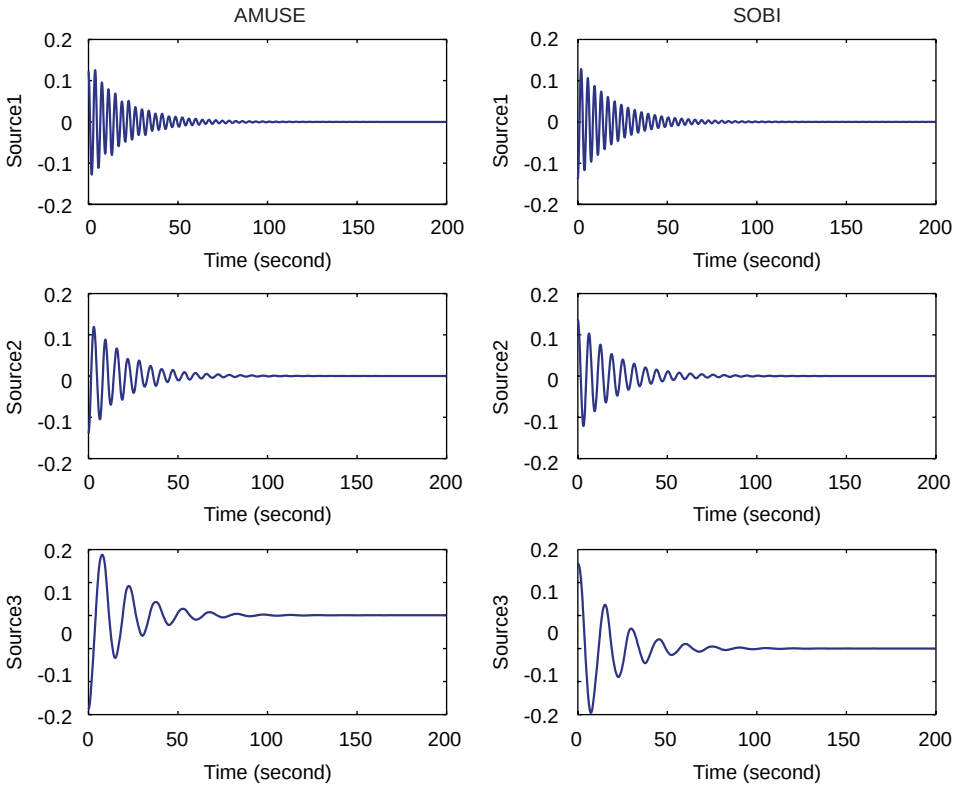

Fig. 6. Separated damped sources from AMUSE and SOBI. Left column represents results from AMUSE and right column gives results from SOBI.

Table 2
Errors of mode shape extraction (damped)

	Er_1 (MAC_1)	Er_2 (MAC_2)	Er_3 (MAC_3)
AMUSE	0.0911 (0.99)	0.0493 (0.99)	0.1311 (0.98)
SOBI	0.0046 (1.00)	0.0306 (0.99)	0.0515 (0.99)
ITD	0.0001 (1.00)	0.0001 (1.00)	0.0000 (1.00)

After applying AMUSE and SOBI to the simulated output displacement signals, we can get the separated sources as it is drawn in Fig. 6. The estimated mixing matrix provides the mode shape information. The results of mode shape extraction are given in Table 2. All the symbols have the same meanings as before.

The added damping ratios affect the performance of the BSS algorithms. AMUSE results suffer the most while SOBI appears more robust than AMUSE. Again ITD provides exact solutions.

4.2. Noisy vibration system

4.2.1. Robustness test on noisy vibration data

In this section, application of the aforementioned algorithms to noisy vibration data without any signal preprocessing is performed. The output displacement responses are contaminated by zero-mean Gaussian white noise. The same simulation setup and parameters as before are used. The signal-to-noise-ratios (SNRs) considered are 11.8323, 8.9503, 12.6611 dB for each of the output channel. We run the Monte Carlo simulation 50 times and plot the results in Fig. 7. Here y-coordinate represents mode shape errors Er between theoretical results and the proposed methods in this simulation. x-coordinate represents the simulation index

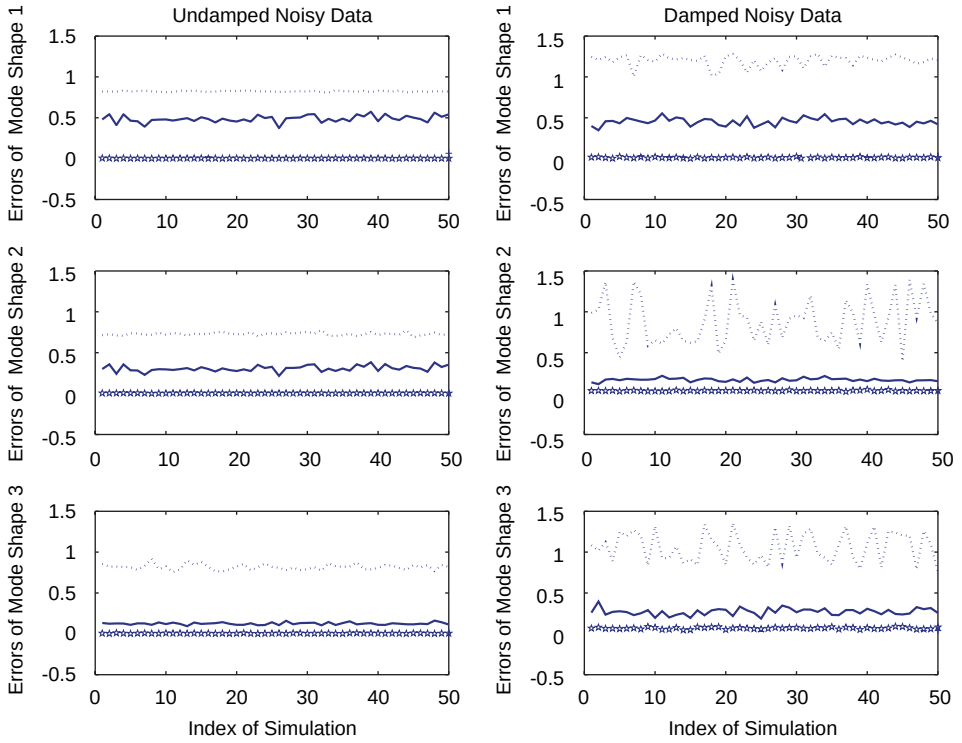

Fig. 7. Comparison of the mode shape extraction in the noisy environment. Left column contains the results for the undamped case. Right column is composed of the results from the damped case. The solid lines represent the results from AMUSE. The dotted lines are from ITD method. Stars (☆) are for SOBI.

Table 3
Errors of mode shape extraction (noisy)

	Method	Er_1 (MAC_1)	Er_2 (MAC_2)	Er_3 (MAC_3)
Undamped	AMUSE	0.4875 (0.81)	0.3069 (0.91)	0.1246 (0.98)
	SOBI	0.0030 (1.00)	0.0043 (1.00)	0.0052 (1.00)
	Ibrahim	0.8230 (0.43)	0.7288 (0.52)	0.8173 (0.44)
Damped	AMUSE	0.4525 (0.83)	0.1674 (0.97)	0.2703 (0.93)
	SOBI	0.0117 (0.99)	0.0346 (0.99)	0.0685 (0.99)
	Ibrahim	1.2001 (0.21)	0.8797 (0.40)	1.0601 (0.31)

for the Monte Carlo simulation. The left column lists the undamped case and the right column gives for the results from damped environment. Table 3 gives the average errors for each mode shape of these methods in the 50 Monte Carlo simulations.

As can be seen from the results, the performance of AMUSE and ITD deteriorate considerably, while SOBI turns out to be robust to noise. The results show that ITD seems to be the worst in the noisy simulation. This is probably because ITD relies on the exact mathematical form of output signals, and when there is noise present in the data, the mathematical model of the data does not hold any more.

4.2.2. Noise reduction on the performance of the algorithms

Most of current time domain modal analysis methods have a common signal preprocessing step which is based on PCA. The effect of this step is to identify noisy subspaces in the signal space and project them out of the signal. Quite similarly, in many BSS algorithms when the number of mixed signals is greater than the

underlying sources, PCA is also performed to identify the number of sources as well as to reduce noise. In this section, this PCA analysis is considered. Instead of extracting mode shapes from the trajectory matrix directly, a higher dimensional matrix $\hat{\mathbf{X}}$ assembled by several time-lagged output matrices is constructed first

$$\hat{\mathbf{X}} = \begin{bmatrix} \mathbf{X}_{\tau} \\ \mathbf{X}_{2\tau} \\ \vdots \\ \mathbf{X}_{k\tau} \end{bmatrix}. \tag{21}$$

Then, PCA is used to examine the noise floor and we project $\hat{\mathbf{X}}$ to a lower dimensional matrix $\tilde{\mathbf{X}}$ according to the noise floor [14]. The reconstructed dimension of the matrix $\hat{\mathbf{X}}$ is chosen as 18 tentatively. The transformed matrix $\tilde{\mathbf{X}}$ has a dimension of 6 by examining the noise floor. With this transformed matrix $\tilde{\mathbf{X}}$, we can perform the same analysis as for the noise free case.

Fig. 8 shows the results of mode shape extraction after 50 Monte Carlo simulations. The left column contains the results from AMUSE and ITD method, while the right column gives results from SOBI. Numerical results are listed in Table 4. As can be seen the results for all algorithms have been improved, among which ITD benefits the most.

4.3. Experimental results

A $0.0063 \times 0.05 \times 0.96\,\mathrm{m}^3$ uniform aluminum beam clamped as fixed-free is used as a test to validate the proposed BSS-based mode shape extraction. Five accelerometers are evenly attached along the beam to measure the responses excited by an impact hammer. All acceleration signals are fed to signal conditioners and

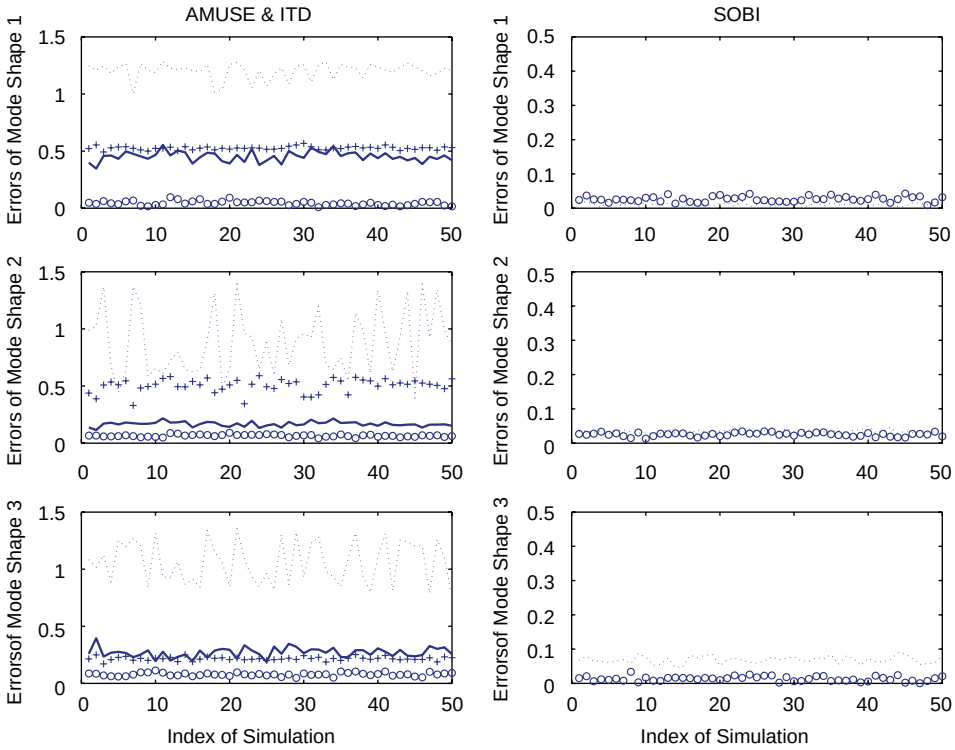

Fig. 8. Comparison of the mode shape extraction before and after PCA preprocessing. Left column are for AMUSE and ITD. The solid lines represent the results from AMUSE without PCA, the dotted lines are from ITD method without PCA, circles (○) and pluses (+) are from both methods after PCA, respectively. Right column is for the case of SOBI. The dotted lines represent the results from SOBI without PCA. Circles (○) are for the results of SOBI after PCA.

Table 4
Errors of mode shape extraction (after PCA)

	Method	Er_1 (MAC_1)	Er_2 (MAC_2)	Er_3 (MAC_3)
Raw	AMUSE	0.4525 (0.83)	0.1674 (0.97)	0.2703 (0.93)
	SOBI	0.0117 (0.99)	0.0346 (0.99)	0.0685 (0.99)
	ITD	1.2001 (0.21)	0.8797 (0.40)	1.0601 (0.31)
Preprocessed	AMUSE	0.0439 (0.99)	0.0646 (0.99)	0.0780 (0.98)
	SOBI	0.0133 (0.99)	0.0265 (0.99)	0.0251 (0.99)
	ITD	0.0526 (0.99)	0.5043 (0.78)	0.2160 (0.94)

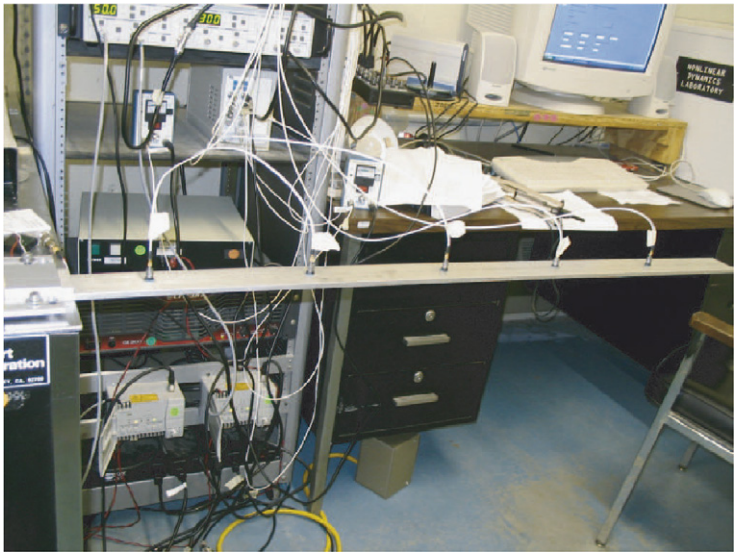

Fig. 9. Picture of laboratory experimental setup.

then to anti-aliasing analog filters. The output signals are sampled digitally by a National Instrument data acquisition board and stored in a PC. The cut-off frequency for all channels are chosen to be 300 Hz. The sampling frequency in the whole experiment is set to 900 Hz. Fig. 9 gives the picture of the experimental setup.

Fig. 10 shows a typical acceleration history (first accelerometer) from tests and its *power spectral density* (PSD). As can be seen, there are five dominant spikes less than 300 Hz, which indicate there are at least five modes excited in the output signals.

Finite element analysis (FEA) of this cantilevered beam is performed first. Six elements according to the locations of the accelerometers are used to model the beam. The five mode shapes described by the locations of the sensors are listed in Table 5. Mode shapes from *Euler–Bernoulli* beam theory are also calculated and the results are very close to the FEA results.

The experimental analysis starts with a step of PCA as described before. Here, we choose to construct a higher dimensional matrix $\hat{\mathbf{X}} \in \mathbb{R}^{30\times1900}$ then project it to a lower dimensional matrix $\tilde{\mathbf{X}} \in \mathbb{R}^{10\times1900}$ based on the noise floor of the matrix $\hat{\mathbf{X}}$. Fig. 11 draws the logarithms of the singular values of $\hat{\mathbf{X}}$, which correspond with the fact that there are five vibration modes in the signals. Each mode is described by a pair of complex conjugates or physically is described in a 2-d phase plane. Modal parameters of the cantilevered beam are obtained by applying SOBI or ITD to the matrix $\tilde{\mathbf{X}} \in \mathbb{R}^{10\times1900}$. Here, only SOBI analysis is performed since it is more robust than AMUSE. The mode shape results from SOBI and ITD are compared to the FEA results and are listed in Table 6. The subscripts S represent SOBI and I represent ITD. As can be seen, with

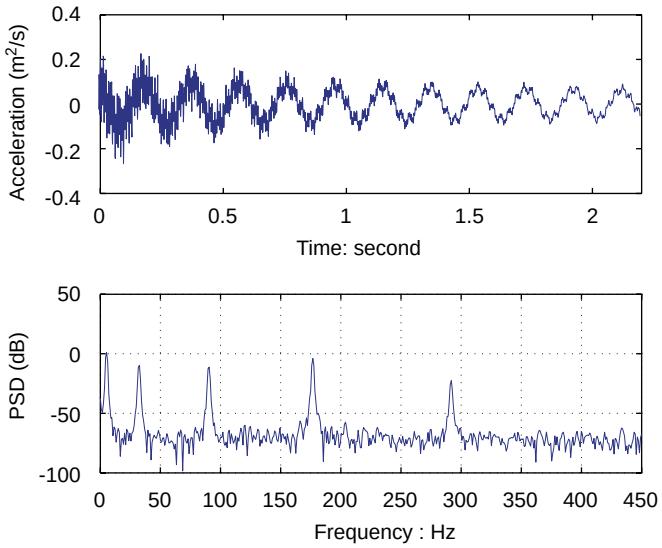

Fig. 10. Experimental signal from accelerometer 1.

Table 5
Mode shape results from FEA

1st	2nd	3rd	4th	5th
0.0111	−0.0596	0.1449	−0.2434	−0.3331
0.1128	−0.4458	0.7079	−0.5821	−0.1520
0.2952	−0.7147	0.2922	0.5371	0.4315
0.5287	−0.5175	−0.5491	0.0912	−0.6024
0.7877	0.1381	−0.3016	−0.5523	0.5628

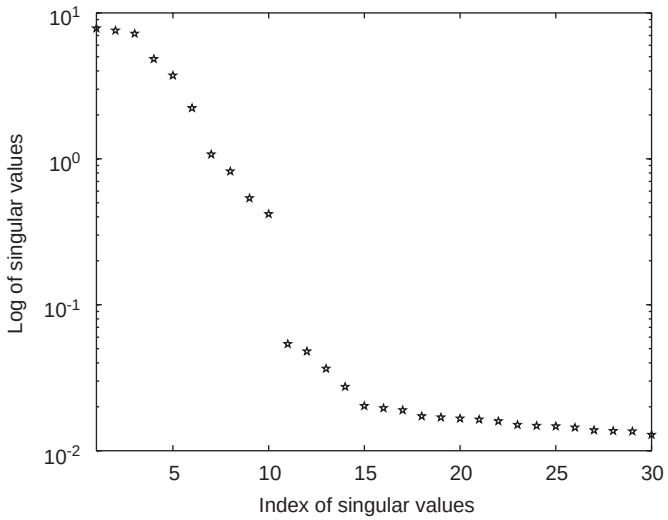

Fig. 11. Noise floor indicated by singular values of $\hat{\mathbf{X}}$.

experimental data containing more or less noise, the mode shape extraction from SOBI are comparable or even better than ITD results. Fig. 12 draws the estimated mode shapes from ITD, SOBI, FEA, and *Euler–Bernoulli* beam theory.

Table 6
Errors of extracted mode shapes between SOBI, ITD and FEA results

	1st	2nd	3rd	4th	5th
Er_S	0.0363	0.0643	0.0860	0.1801	0.4317
Er_I	0.0327	0.0684	0.0852	0.1792	0.4607
MAC_S	0.9987	0.9959	0.9926	0.9678	0.8223
MAC_I	0.9989	0.9953	0.9928	0.9681	0.7990

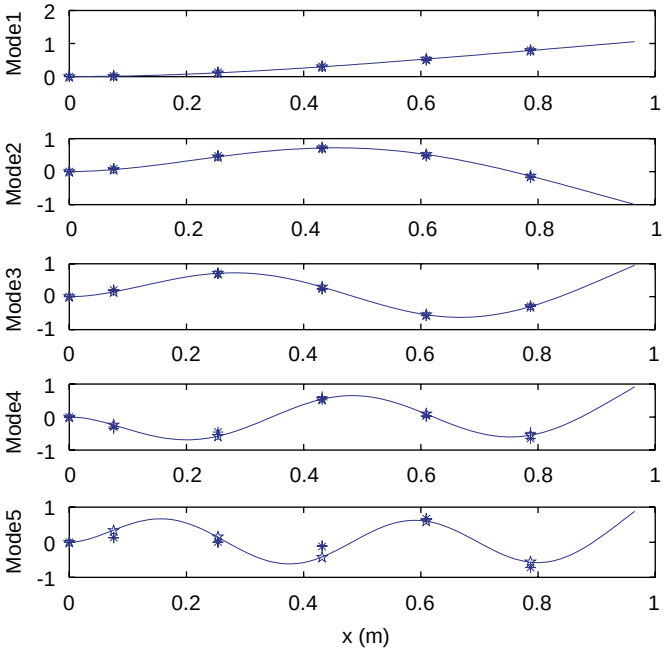

Fig. 12. Comparison of mode shapes from SOBI, ITD, FEA and *Euler–Bernoulli* beam theory. Continuous lines represent mode shapes from beam theory, "$*$" represent results from SOBI, "+" are from ITD analysis and "$\star$" are from FEA.

5. Discussion and conclusion

Above we have talked about mode shape extraction by using only output signals. After separation, independent modal coordinates can be recovered by using mixing (mode shape) matrix and vibration signals. From each modal coordinates, we can apply traditional FFT and Hilbert-envelope method to extract frequencies and damping ratios. If the obtained vibration signals are noise free, the estimation is usually good. For example, in the previous example (Section 4.1.1) the theoretical natural frequencies are: 0.0670, 0.1592, 0.2675 Hz. Estimated natural frequencies from SOBI are: 0.0684, 0.1612, 0.2687 Hz (the maximum error is 2.0% for the first natural frequency). For the example in Section 4.1.2, the estimated damping ratios are: 0.1141, 0.0484, 0.029 (the maximum error is 4.9% for the first damping ratio) obtained by examining the decay rates of each separated source after Hilbert transformation. When vibration signals are noisy, modal coordinate extraction through BSS is also noisy. Therefore the estimation of natural frequencies and damping ratios is less accurate according to noisy modal coordinates. In the experimental example (Section 4.3), calculated frequencies from FEA and Euler–Bernoulli theory are: 5.62, 35.25, 99.01, 195.61, and 324.66 Hz. The frequencies from SOBI are: 5.25, 32.51, 90.50, 176.70, and 291.70 Hz. ITD gives the frequencies as: 5.15, 32.23, 90.24, 176.75, 291.82 Hz. The experimental results (both SOBI and ITD) do not match with theoretical result well, especially for the 5th mode the error is 10.12%. The causes are possibly due to noisy modal coordinates, approximation of ideal fix-free boundary condition and modeling error, etc. Damping ratios from SOBI are: 0.0060, 0.0028, 0.0019, 0.0014, 0.0014 and from ITD are: 0.0335, 0.0021, 0.0019, 0.0015,

0.0014. Future work could be done in robustly extracting frequencies and damping ratio from noisy modal coordinates.

Applications of BSS to the identification of modal parameters, especially mode shapes, were presented in this paper. Viewing from the BSS point of view, conventional time domain modal analysis can be achieved by extracting independent oscillations and a mixing matrix from output signals. The mixing matrix contains mode shape information, and natural frequencies and damping ratios can be further identified from each independent oscillation. In practical vibration tests, acceleration signals are more often measured. However, this should not affect the results of this study, since compared with displacement signals acceleration signals introduce only phase and amplitude changes while not changing the mixing procedure. This has been verified in the above experiment example, where the outputs are accelerations. The proposed BSS-based mode shape extraction should be classified as an output-only method, which can extract modal parameters without knowing input information. The output-only modal analysis methods have certain advantages over traditional frequency domain methods in practical tests where detailed inputs are not readily available. In this paper, we examined ITD method and did the comparison since AMUSE and SOBI have quite similar steps to ITD. Simulation results show better performance of SOBI in noisy environment over ITD when extracting mode shapes. Recently, we have learned that Kerschen et al. are conducting similar research in BSS-based modal analysis. Some of the progress can be seen in Ref. [27].

In conclusion, in this paper BSS algorithms are proposed to extract LNMs from vibration systems. AMUSE from BSS and ITD from time domain modal analysis are examined to show the similarity between the two different problems. Numerical and experimental results show BSS algorithms can robustly identify LNMs with only output signals (displacement or accelerations).

Acknowledgments

The work presented in this paper was supported by the National Science Foundation under Grant No. 0237792.

References

[1] A. Hyvarinen, J. Karhunaen, Erkki Oja, Independent Component Analysis, Wiley, New York, 2001.
[2] J. Fortuna, D. Capson, ICA for position and pose measurement from images with occlusion, in: Proceedings of the IEEE International Conference on Acoustics, Speech, and Signal Processing, (ICASSP '02), vol. 4, 2002, pp. 3604–3607.
[3] A. Cichocki, Blind signal processing methods for analyzing multichannel brain signals, International Journal of Bioelectromagnitism 6 (1) (2004) 22–27.
[4] U. Madhow, Blind adaptive interference suppression for direct-sequence CDMA, Proceedings of the IEEE 86 (10) (1998) 2049–2069.
[5] E. Oja, K. Kiviluoto, S. Malaroiu, Independent component analysis for financial time series, in: Adaptive Systems for Signal Processing, Communications, and Control Symposium 2000, AS-SPCC, The IEEE 2000, Lake Louise, Alta, 2000, pp. 111–116.
[6] C. Zang, M.I. Friswel, M. Imregun, Structural damage detection using independent component analysis, Structural Health Monitoring 3 (1) (2004) 69–83.
[7] R. Peled, S. Braun, M. Zacksenhouse, A blind deconvolution separation of multiple sources with application to bearing diagnostics, Mechanical Systems and Signal Processing 19 (6) (2005) 1181–1195.
[8] C. Serviere, P. Fabry, Blind source separation of noisy harmonic signals for rotating machine diagnosis, Journal of Sound and Vibration 272 (1–2) (2004) 317–339.
[9] G. Gelle, M. Colas, G. Delaunay, Blind source separation applied to rotating machines monitoring by acoustical and vibrations analysis, Mechanical Systems and Signal Processing 14 (3) (2000) 427–442.
[10] S.R. Ibrahim, E.C. Mikulcik, A time domain modal vibration test technique, The Shock and Vibration Bulletin 43 (4) (1973) 21–37.
[11] J.N. Juang, R.S. Pappa, An eigensystem realization algorithm for modal parameter identification and model reduction, Journal of Guidance, Control and Dynamics 8 (5) (1985) 620–627.
[12] D.L. Brown, R.J. Allemang, R. Zimmerman, M. Mergeay, Parameter estimation techniques for modal analysis, SAE Technical Paper Series 790221, 1979, pp. 15–24.
[13] H. Vold, J. Kundrat, G.T. Rocklin, R. Russel, A multi-input modal estimation algorithm for mini-computers, SAE Technical Paper Series 820194, 1982, pp. 828–841.
[14] S.R. Ibrahim, E.C. Mikulcik, A method for the direct identification of vibration parameters from the free response, The Shock and Vibration Bulletin 47 (4) (1977) 183–198.
[15] L. Tong, R.W. Liu, V.C. Soon, Y.F. Huang, Indeterminacy and identifiability of blind identification, IEEE Transactions on Circuits and Systems 38 (5) (1991) 499–509.

[16] A. Belouchrani, K. Abed-Meraim, J.F. Cardoso, E. Moulines, A blind source separation technique using second-order statistics, IEEE Transactions on Signal Processing 45 (2) (1997) 434–444.
[17] A. Taleb, C. Jutten, Source separation in post-nonlinear mixtures, IEEE Transactions on Signal Processing 47 (10) (1999) 2807–2820.
[18] N. Delfosse, P. Loubaton, Adaptive blind separation of independent sources: a deflation approach, Signal Processing 45 (1) (1995) 59–83.
[19] G.R. Ayers, J.C. Dainty, Iterative blind deconvolution method and its applications, Optics Letters 13 (7) (1988) 547–549.
[21] J.F. Cardoso, E. Oja, Eigen-structure of the fourth-order cumulant tensor with application to the blind source separation problem, in: International Conference on, Acoustics, Speech, and Signal Processing, ICASSP-90, 1990, ALbuquerque New Mexico, pp. 2655–2658.
[22] A. Hyvarinen, E. Oja, A fast fixed-point algorithm for independent component analysis, Neural Comput. 9 (7) (1997) 1483–1492.
[23] J.F. Cardoso, Infomax and maximum likelihood for blind source separation, Signal Processing Letters IEEE 4 (4) (1997) 112–114.
[24] A. Ziehe, H.B. Muller, TDSEP—an efficient algorithm for blind separation using time structure, in: Proceedings of ICANN, vol. 98, 1998, pp. 675–680.
[25] A. Belouchrani, M.G. Amin, Blind source separation based on time frequency signal representation, IEEE Transactions on Signal Processing 46 (11) (1998) 2888–2897.
[26] W. Zhou, Multivariate analysis on vibration modal analysis, Ph.D. Dessertation, University of Rhode Island, 2006.
[27] G. Kerschen, F. Poncelet, J.-C. Golinval, Physical interpretation of independent component analysis in structural dynamics, Mechanical Systems and Signal Processing 21 (4) (2007) 1561–1575.